GEOMATICS, NATURAL HAZARDS AND RISK, 2017
VOL. 8, NO. 2, 1792–1811
https://doi.org/10.1080/19475705.2017.1388853

Taylor & Francis
Taylor & Francis Group

OPEN ACCESS Check for updates

Application of remote sensing and GIS-based hydrological modelling for flood risk analysis: a case study of District 8, Ho Chi Minh city, Vietnam

An Thi Ngoc Dang and Lalit Kumar

School of Environmental and Rural Science, University of New England, Armidale, Australia

ABSTRACT
Rapid and unplanned urbanization, together with climate change, have exacerbated flood risk which has caused devastating loss of human life and property in Ho Chi Minh City, Vietnam. Our study utilized remote sensing techniques combined with Geographic Information Systems-based hydrological modelling to identify flood risk in this urban area. QuickBird imagery was used to create land-use/land-cover information, an important input into the U.S. Soil Conservation Service Technique Release 55 (SCS TR-55) model which is used for predicting rainfall-induced flood. Tidal floods were examined using a Digital Elevation Model in a GIS framework with water level in rivers as an input. The findings indicated that rainfall-induced flood is not a serious problem with the flood depth of 2–10 cm while tidal flood is a substantial issue with 10–100 cm flood depths. Increasing impervious surfaces and decreasing flow length areas resulting from the growth of urbanization in combination with tidal effects contributed significantly to increased flood risk. These findings have implications on solutions for flood risk control in the district, including managing urbanization processes with appropriate infrastructure and improving the infiltration capacity of the runoff with optimized drainage systems.

ARTICLE HISTORY
Received 24 November 2016
Accepted 16 September 2017

KEYWORDS
Remote sensing; GIS; DEM; hydrological model; flood hazard; flood map; SCS TR-55 model; spatial analysis

1. Introduction

Ho Chi Minh City (HCMC) is among the cities that are most at risk of flooding worldwide (Eckert 2011; Hanson et al. 2011; Hallegatte et al. 2013). It is located on the edge of the Mekong Delta and built mostly on marshy, low-lying land (Eckert 2011). Over 60% of the administrative area is located below 1.5 m above mean sea level (Long 2007) and consists of an extensive network of canals and rivers (Nguyen and Tung 2007). In addition, the tidal intrusion into the urban water systems causes periodic rises in water level (Lempert et al. 2013). Such geographic features, combined with periods of intense rainfall and upstream areas, mean the city is facing a frequent and significant flood risk (Storch and Downes 2011; Lempert et al. 2013). Climate change has also exacerbated the risks of inundation in HCMC (Carew-Reid 2008; Nicholls et al. 2008; Hanson et al. 2011). During the last 100 years, HCMC has experienced a rise in sea level of around 1 m resulting in the inundation of approximately half of the city and endangering nearly 12% of the population, or 660,000 city residents (Carew-Reid 2008). Furthermore, the rapid growth of the city and expansion of the population, which include many residents with lower socio-economic circumstances, will increase the

---

CONTACT An Thi Ngoc Dang dtngarsc@gmail.com

© 2017 The Author(s). Published by Informa UK Limited, trading as Taylor & Francis Group.
This is an Open Access article distributed under the terms of the Creative Commons Attribution License (http://creativecommons.org/licenses/by/4.0/), which permits unrestricted use, distribution, and reproduction in any medium, provided the original work is properly cited.

economic, social and environmental impacts of flood phenomenon in the future (Ho 2008; Lempert et al. 2013).

Geographic Information Systems (GIS) are important as common data analysis frameworks in modelling (Tianhong et al. 2003; Shen et al. 2005). In hydrological modelling specifically, GIS can be used to construct flooding projection models in catchments, and to prepare and analyse multi-scale and multi-source spatial data (Merwade et al. 2008; Gallegos et al. 2009). When creating hydrological models to investigate flood hazards in catchments, Digital Elevation Models (DEMs) are used in a GIS background to acquire essential topographical variables such as stream networks, flow direction, catchment geometry and slope from raster data on elevation (Tarboton and Ames 2001; Siart et al. 2009). GIS is a critical tool used to project both qualitative and quantitative impacts of floods and runoff (Sivertun and Prange 2003; Sdao et al. 2010; Huong and Pathirana 2013), and GIS-based hydrological models have been successfully utilized for flood prediction in urban areas (Seeni Mohd and Mansor 2000; Samarasinghea et al. 2010; Sarker and Sivertun 2011; Uddin et al. 2013).

GIS in combination with remote sensing (RS) techniques are an efficient tool for analysis, including in identifying flood risk zones and flood impacts on inundated areas (Seeni Mohd and Mansor 2000; Samarasinghea et al. 2010; Sarker and Sivertun 2011; Isma'il and Opeluwa Saanyol 2013; Uddin et al. 2013). RS provides a critical source of data (Seeni Mohd and Mansor 2000; Samarasinghea et al. 2010; Dano Umar et al. 2011), saving both time and manpower in topographical and geomorphological catchment data collection and data analysis (Nicandrou et al. 2004; Nicandrou 2011). GIS combined with RS can also be applied to acquire spatial information in digital form, such as soil type and land-use/land-cover (LULC) variables particularly important for hydrological modelling and flood studies (Seeni Mohd and Mansor 2000; Samarasinghea et al. 2010). RS techniques can be used to analyse satellite imagery and enable more accurate classification of LULC (Nicandrou et al. 2004; Nicandrou 2011). These techniques have been used effectively in a variety of studies to support hydrological models and predict flood risk including Seeni Mohd and Mansor (2000); Samarasinghea et al. (2010); Chowdhury (2000) and Wang et al. (2010).

The Soil Conservation Service Curve Number (SCS-CN) method was developed by the United States Department of Agriculture (USDA) in 1954. The SCS-CN method uses the CN method to estimate direct runoff from storm rainfall. This method determines CN values based on watershed's soil and cover conditions which represent the hydrological soil group, cover type, land-use treatment strategies and hydrological condition, and the direct runoff is determined based on the CN values (USDA 1986). Technique Release 55 (TR-55) is a commonly used hydrological model. This model uses runoff depth data obtained from SCS-CN as an input to determine the peak discharge of watersheds and enables the model to effectively simulate runoff and peak discharge to identify flood phenomenon in urban areas (Seeni Mohd and Mansor 2000; Holman−Dodds et al. 2003; Ramana 2014). The SCS-CN method, as included in TR-55, is widely used for predicting direct runoff volume for a given rainfall event, especially in urban areas (Kim et al. 2010; Dawod et al. 2011; Soulis and Valiantzas 2011; Gajbhiye and Mishra 2012). A number of studies have found that the SCS-CN method is the most effective method for determining runoff volume and peak discharge, examples include Kim et al. (2010); Soulis and Valiantzas (2011); Dawod et al. (2011); Gajbhiye and Mishra (2012) and Shadeed and Almasri (2010).

A particularly formative study by Seeni Mohd and Mansor (2000) used the SCS TR-55 model in integration with GIS tools to estimate urban floods for small watersheds. The results obtained from this study were so effective that they have promoted the use of RS techniques combined with hydrological models, particularly SCS TR-55, for flood prediction in urban areas. Other studies found that this combination of the TR-55 model with GIS sufficiently enhanced the process of estimating runoff volume and peak discharge and was more accurate and quicker than other approaches, by validating their results with observed runoff (Holman−Dodds et al. 2003; Ramana 2014).

Despite a concerted effort to investigate and address the problem of flood risk in HCMC (Ho 2008; Long et al. 2010; Lempert et al. 2013), only a few studies have used GIS and hydrological models to evaluate flood risk in this city. Long (2007) applied GIS in combination with a Storm Water Management Model to quantify the impacts of climate changes on flooding and assess mitigation alternatives. Long et al. (2010) used the Mike Flood Model to evaluate and forecast flooding in HCMC, which better informed management of the flooding potential in the area and resulted in reduced resources spent on flood management and improved efficiency of water drainage.

Despite these studies, there is a knowledge gap of flood risk management and research for HCMC. Despite efforts to reduce flooding in HCMC, conditions have changed since the initial flooding predictions and HCMC is still subject to flooding (Lempert et al. 2013). It has even been suggested that new areas are being increasingly flooded (Long 2007; Ho 2008). Previous studies of flood risk have limitations, such as not taking into account the overall properties of the whole basin, ignoring the underlying causes leading to the flooding, and not realizing that the current rate of urbanization is quickly reducing the drainage capacities of the existing canals (Long et al. 2010). Additionally, studies did not take into account climate change, which is leading to extreme rainfall with over 100 mm rainfall in three hours, as observed at the rain gauge located at HCMC airport during the period of 1961–2007 (Dahm 2013); rising sea levels and higher peak tides than have been seen historically may increase the risk of flooding in HCMC (Long et al. 2010).

If the conditions used to predict flooding are not updated, then current flood predictions of gauged catchments are unlikely to be any more accurate than those used previously. Climate change will likely lead to more excessive flooding events over the coming decades; however, there is high uncertainty around the accuracy of these predictions (Field 2012). Future socio-economic circumstances may also affect flood risk. Cities with emerging economies, such as HCMC, are developing at exceptionally fast rates, further affecting the ability to accurately forecast flooding in a highly dynamic environment (Lempert et al. 2013).

Given the efficacy of RS and GIS-based hydrological modelling, especially the SCS TR-55 model, for flood risk analysis and the changing flood dynamics of HCMC, we used RS techniques combined with GIS and the SCS TR-55 hydrological model to evaluate the flood risk for District 8 of HCMC. This approach will address the above knowledge gaps in flood risk prediction and provide a real scientific basis for forecasting floods for District 8 based on current infrastructure of the city as well as updated climate factors, including rainfall and sea level. This study:

- Examines how RS techniques can be combined with GIS-based hydrological modelling for flood prediction mapping in urban areas in HCMC. Whilst this type of modelling is recommended for flood prediction, it has not been utilized in HCMC.
- Identifies the flood prone areas and flood depth maps in the case study area of District 8, HCMC.
- Provides analysis and the results of different factors affecting floods to the appropriate authorities for use in developing infrastructure to manage flood risk.

1.1. Study area description – District 8, Ho Chi Minh City

The study area, District 8, is located in the south-west of HCMC, between 10°45′08″N, 106°35′51″E and 10°41′45″N, 106°41′22″E. This District is elongate in shape and oriented north-east–south-west, covering an area of 1880 ha. Its topography is heavily dissected by a high density system of rivers (Xuan 2014a) (Figure 1 – source: Vietnam GIS (2014)). The District is characterized by flat topography with a terrain slope of less than 0.1%. Its average elevation is 1.2 m above mean sea level, which is lower than many other districts in HCMC (Xuan 2014a). Two-thirds of District 8 is located below the level of the highest tides ever recorded (1.6 m in November 2011). Parts of the district seriously affected by high tides include the lowland areas of Ward 6, 7, 15 and 16 (Xuan 2014a). The combination of the geography, topography and high density system of rivers and canals means District 8 is one of the most vulnerable areas in HCMC to flooding induced by tidal fluctuations. The centre of the district is highly developed but older in comparison to other areas, thereby

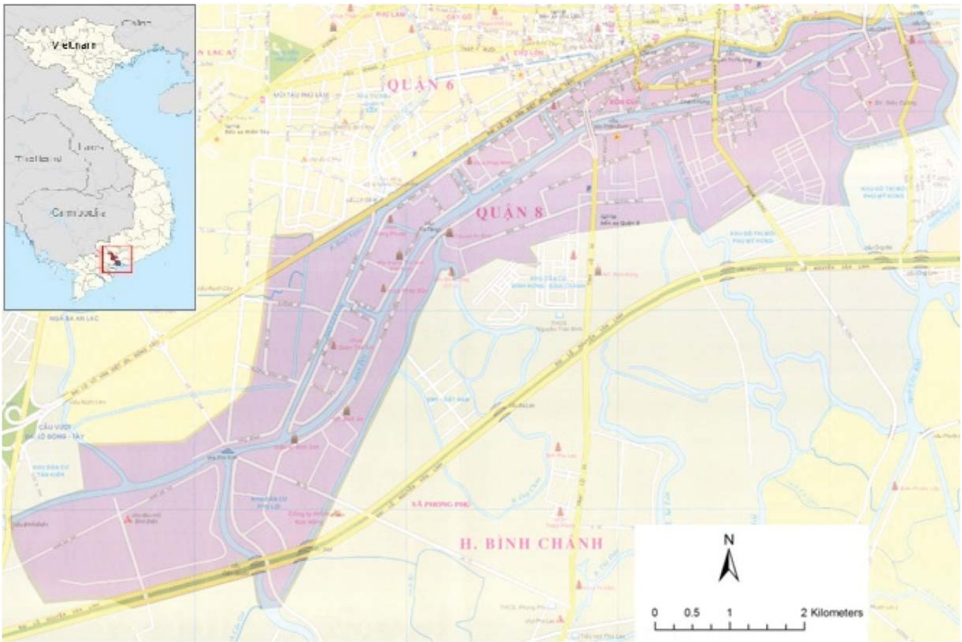

Figure 1. Location of study area, District 8, in Ho Chi Minh City Vietnam, and network of canals shown in blue. Source: Vietnam GIS (2014).

infrastructure, such as pipe systems for discharging runoffs, are old and ineffective and this can accelerate flooding.

2. Materials and methods

2.1. Materials

QuickBird imagery was selected to produce LULC and impervious areas layers, which were extracted as an input parameter for the hydrological model in this study (Figure 2).

GIS data used in this study included topographical database, soil type data and DEM. The data were collected from the Department of National Remote Sensing, Vietnam. The topographical database includes objects such as buildings and constructions, traffic route networks, LULC, water systems, administrative borders and elevation. Soil type data were used in the hydrological model to calculate runoff volume and peak discharge. DEM at 2 m resolution was utilized to delineate sub-catchments, to parameterize sub-catchments for the hydrological model and to identify flood-induced tide.

Daily rainfall was highly variable during the observation period. TR-55 model uses amount of rainfall based on 24-hour storm events as an input to estimate rainfall runoff. Based on this approach, the highest rainfall amount of 3.59 inches, based on 24-hour storm events, was applied to represent the highest risk of flooding, and this rainfall amount has occurred with high frequency in recent years. This rainfall amount was obtained from the rainfall records obtained from the Southern Regional Hydro-Meteorological Centre.

Data of water level in rivers was obtained from PhuAn meteorological station located on the Sai Gon River which is connected to the rivers and canals in the case study site and approximately 2 kilometres from this study area. Therefore, PhuAn station was ideal for water level observation data for the case study site. The highest values of water level in rivers were used to predict the risk of induced tide flood; these values occurred with the highest frequency in the case study site in 2010.

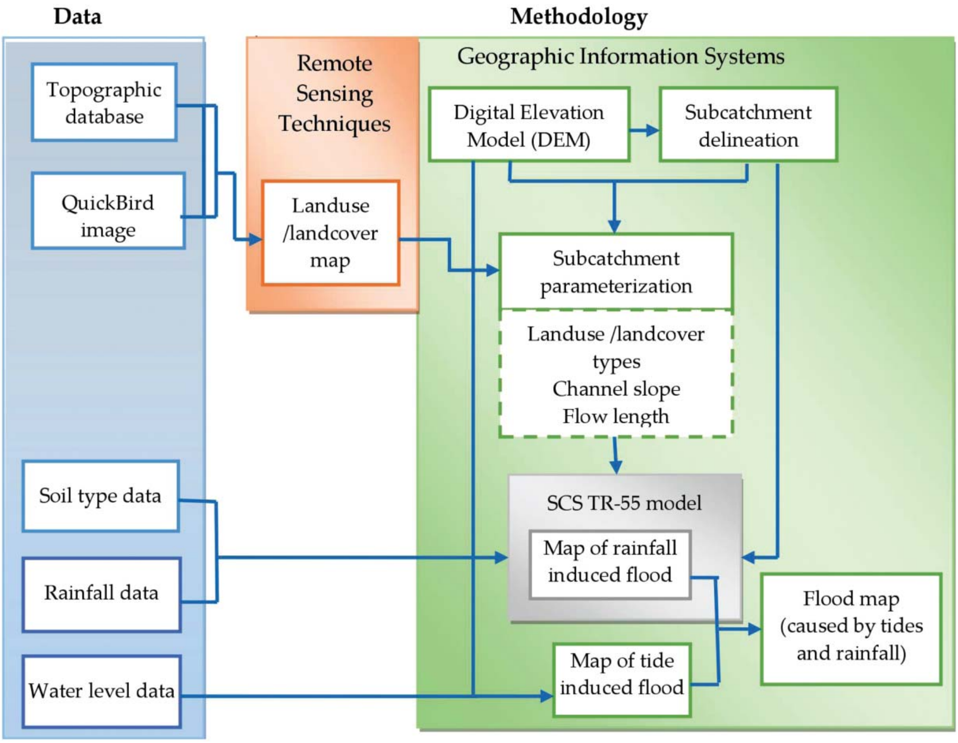
Data
Methodology
Topographic database
QuickBird image
Remote Sensing Techniques
Landuse /landcover map
Geographic Information Systems
Digital Elevation Model (DEM)
Subcatchment delineation
Subcatchment parameterization
Landuse /landcover types
Channel slope
Flow length
SCS TR-55 model
Map of rainfall induced flood
Soil type data
Rainfall data
Water level data
Map of tide induced flood
Flood map (caused by tides and rainfall)

Figure 2. Flowchart showing the methodology used in this study.

2.2. Methods

2.2.1. Remotely sensed data processing

The QuickBird scene (Figure 3) was geometrically referenced using 15 Ground Control Points (GCPs) to UTM map projection (UTM-48 N, WGS-84 datum). The GCPs were taken from topographical maps of the study area at a 1:2000 scale. Cubic Convolution Interpolation was then applied to the QuickBird image using geometric correction to smoothen and sharpen the image. Due to the low topographical variation of HCMC, a topographical correction of the QuickBird image was not necessary (Vo et al. 2013).

Image classification was carried out to classify the LULC types in the study area, thereby creating a LULC map of land-use types (Figure 3) to be used in the TR-55 model. A Maximum Likelihood

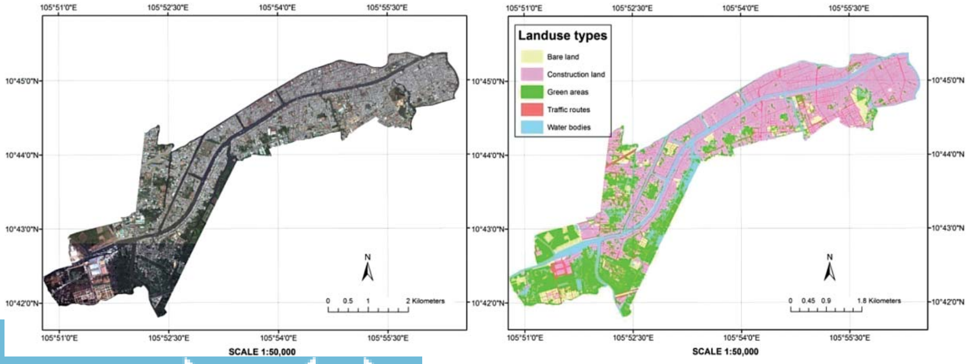
105°51'0"E
105°52'30"E
105°54'0"E
105°55'30"E
10°45'0"N
10°44'0"N
10°43'0"N
10°42'0"N
N
0 0.5 1 2 Kilometers
SCALE 1:50,000
Landuse types
Bare land
Construction land
Green areas
Traffic routes
Water bodies
0 0.45 0.9 1.8 Kilometers
SCALE 1:50,000

Figure 3. QuickBird image (left) and land-use/land-cover map (right) of District 8 of HCMC, Vietnam.

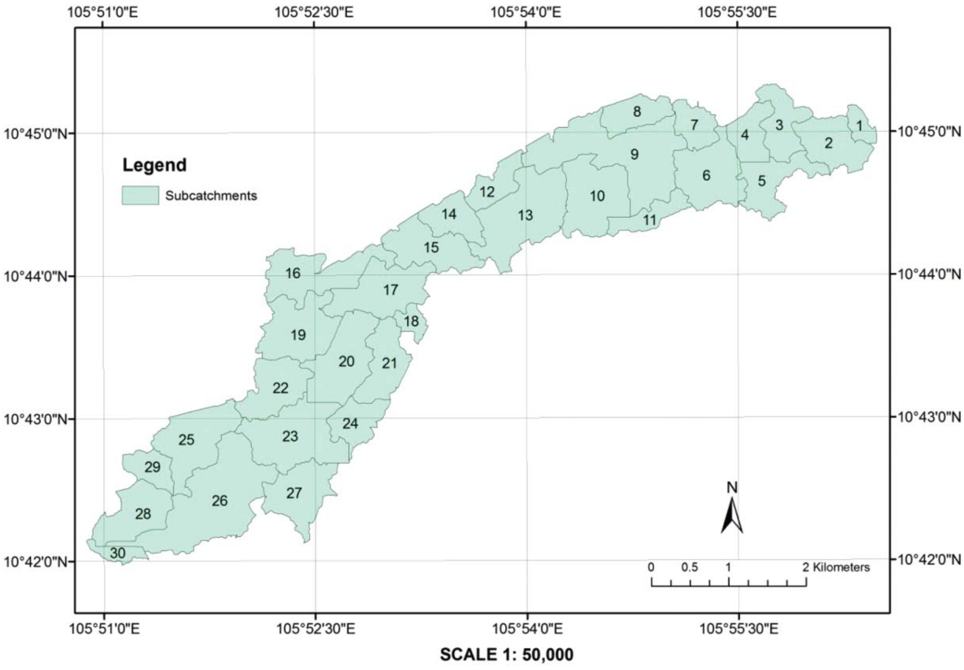

Figure 4. Sub-catchments in District 8, Ho Chi Minh City, Vietnam.

Algorithm was used for classification in which the classification was based on the number of training samples identified from topographical maps and LULC maps. Five classes of LULC were identified: (1) water bodies (rivers, streams, lakes, canals); (2) traffic routes (roads, pavement, concrete, airport runways); (3) construction land (including land for residential development, houses, public service places, public administration); (4) bare land (unplanted land, excluding concrete transport roads); (5) green areas (vegetables, rice paddy fields and grass/ parks). The overall classification accuracy was 85%.

Visual interpretation and editing was used to tackle the misclassification problem to improve the accuracy of the map for further use in the TR-55 model.

2.2.2. Sub-catchment delineation

The case study area was divided into 30 small sub-catchments using the hydrological tools in ArcGIS software with DEM as an input, so as to provide sufficient detail to support the SCS TR-55 model. Sub-catchments were delineated from 2 m DEM by computing the flow direction grid and flow accumulation grid (with threshold value of 12,500 cells or 50 ha) by using Flow Direction tool and Flow Accumulation tool, respectively (ESRI 2012). After this, the pour points for the sub-catchments were added based on the flow accumulation grid to be the junctions of a stream network derived from flow accumulation to divide the case study into small sub-catchments. The details pertaining to the delineated sub-catchments are shown in Figure 4.

2.2.3. Sub-catchment parameterization

ArcGIS software was used to calculate the parameters of the sub-catchments that were used as input for the SCS TR-55 model used for identifying the flood risk to HCMC. The parameters were LULC type, flow length and channel slope.

LULC types within each sub-catchment were used as parameters for estimating the CN values for each sub-catchment. The Zonal Statistics as Table Tool (ESRI 2012) was used to identify the forms of LULC within each sub-catchment with LULC map as an input. Table 1 gives the data and software used in the modeling.

Table 1. Data and softwares used in this project.

Data	Spatial resolution (m)	Date	Software
QuickBird image	0.65 × 0.65 (pan)	2010	Envi, ArcGIS
Topographical database		2008	ArcGIS
Water level of rivers data		2010	ArcGIS
Rainfall data		2010	ArcGIS
Soil type data		2010	ArcGIS
DEM		2008	ArcGIS

Channel slope and flow length were the parameters used to calculate the time of concentration (conceptual) for calculating both the runoff and peak discharge for sub-catchments. These two parameters were calculated using an extension of ESRI's ArcGIS: the Hydrological Engineering Centre's Geospatial Hydrological Modelling System (HEC-GeoHMS) (Fleming and Doan 2009) with DEM as an input.

2.2.4. Application of SCS TR-55 model for rainfall induced flood

In this study, the hydrological model SCS TR-55 was applied to investigate rainfall-induced flood phenomenon. It is a simple method which can be used to forecast both runoff and peak discharge in small sub-catchments. To determine flood occurrence, we compared the values of peak discharge to the values of bankfull discharge, with flooding occurring if the peak discharge exceeded the bankfull discharge. This required calculating peak discharge and bankfull discharge as shown in the following.

2.2.4.1. Determination of peak discharge.

(1) Determination of runoff

The following equations were used in the SCS TR-55 model to determine runoff, based on the USDA (1986).

$$Q = \frac{(P - I_a)^2}{(P - I_a) + S} \tag{1}$$

where Q = runoff (in), P = rainfall (in), S = potential maximum retention after runoff begins (in) and I_a = initial abstraction (in).

Initial abstraction (I_a) is lost before runoff begins (includes water retained in surface depressions; water intercepted by vegetation, evaporation and infiltration).

I_a is highly variable but is generally correlated with soil and cover parameters.

I_a was approximated by the following empirical equation (USDA 1986):

$$I_a = 0.2\,S \tag{2}$$

Removing I_a as an independent parameter by substituting Equation (2) into Equation (1) gives

$$Q = \frac{(P - 0.2\,S)^2}{(P + 0.8\,S)} \tag{3}$$

S is linked to the soil and cover conditions of the sub-catchments through the CN, has a range of 0–100 and is related to CN by

Table 2. Curve number (CN) values for each land cover in the case study area of Ho Chi Minh City (USDA 1986).

Land-cover/land-use	CN for hydrological soil group – B
Water body	100
Urban or built-up area	93
Street and roads	98
Grassland	65
Bare soil	86

$$S = \frac{1000}{\mathrm{CN}} - 10 \tag{4}$$

Based on the SCS TR-55 model, the runoff CN for the soil type and land-cover conditions of the sub-catchments in the case study area is as provided inTable 2.

The sub-catchments in the case study had complex land-use and land-cover, so the CN values of the sub-catchments were identified using average CN values method as described in the following.

As catchments with sub-areas experience various types of land-use and land-covers, a composite CN is determined by weighting the CN values for the different sub-areas in proportion to the land area associated with each (Shadeed and Almasri 2010).

$$\mathrm{CN}_c = \frac{\mathrm{CN}_1 A_1 + \mathrm{CN}_2 A_2 + \cdots + \mathrm{CN}_i A_i + \cdots + \mathrm{CN}_n A_n}{\sum_{i-1}^{n} A_i} \tag{5}$$

where CN_c is composite curve number, CN_i is the curve number of the sub-area i, A_i is the area of the sub-area i and n is the total number of sub-areas.

Figure 5 shows CN values of the sub-catchments in the case study.

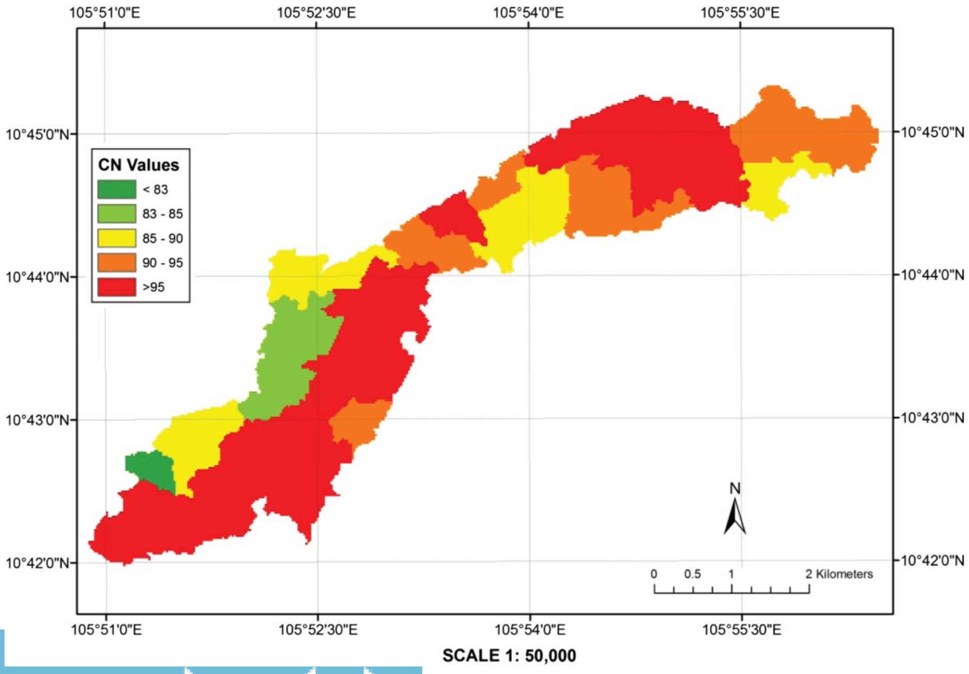

Figure 5. CN values of sub-catchments in District 8, Ho Chi Minh City, Vietnam.

(2) Computation of travel time and time of concentration

Travel time (T_t) is the time that water takes to travel from one location to another in a watershed. T_t is the ratio of flow length to flow velocity and is a component of time of concentration (T_c); the time for runoff to travel from the hydraulically most distant point of the watershed to a point of interest within the watershed. T_c is computed by summing all the travel times for consecutive components of the drainage conveyance system. These values are calculated using the following equation (USDA 1986):

$$T_t = \frac{L}{3600\mathrm{V}} \tag{6}$$

where T_t = travel time (hour), L = flow length (ft), V = average velocity (ft/s), 3600 = conversion factor from seconds to hours.

The average velocity (V) is computed using the Manning equation:

$$V = \frac{1.49 r^{2/3} s^{1/2}}{n} \tag{7}$$

where V = average velocity (ft/s), r = hydraulic radius (ft), s = slope of the hydraulic grade line (channel slope, ft/ft) and n = Manning's roughness coefficient for open channel flow. For unpaved areas, n is 0.05 and r is 0.4; for paved areas, n is 0.025 and r is 0.2 (USDA 1986).

Time of concentration (T_c) is the sum of T_t values for the various consecutive flow segments:

$$T_c = T_{t1} + T_{t2} + \cdots + T_{tm} \tag{8}$$

where T_c = time of concentration (hour), and m = number of flow segments.

(3) Determination of peak discharge

The peak discharge is computed by the SCS TR-55 graphical method, in which the peak discharge is calculated by

$$q_p = q_u A_m Q F_p \tag{9}$$

where q_p = peak discharge (cfs), q_u = unit peak discharge (csm/in), A_m = drainage area (mi^2), Q = runoff (in) and F_p = pond and swamp adjustment factor.

The value for q_u is obtained from the Unit Peak Discharge graph for SCS type II rainfall distribution as shown in Figure 6 (USDA 1986). This type of rainfall distribution was selected to calculate q_u for the case study because this type of rainfall is characterized by most intense short duration rainfall and is most relevant to rainfall style in the case study site.

2.2.4.2. Determination of bankfull discharge. The bankfull discharge was calculated using the following equation (Department of Water Sanitation and Environment 2008):

$$q_b = A \times \frac{1 + C \times \log P}{(t + b)^n} \tag{10}$$

where q_b = bankfull discharge (m^3/s), A = 11,650, C = 0.58, b = 32, n = 0.95, P = 2 years (2-year

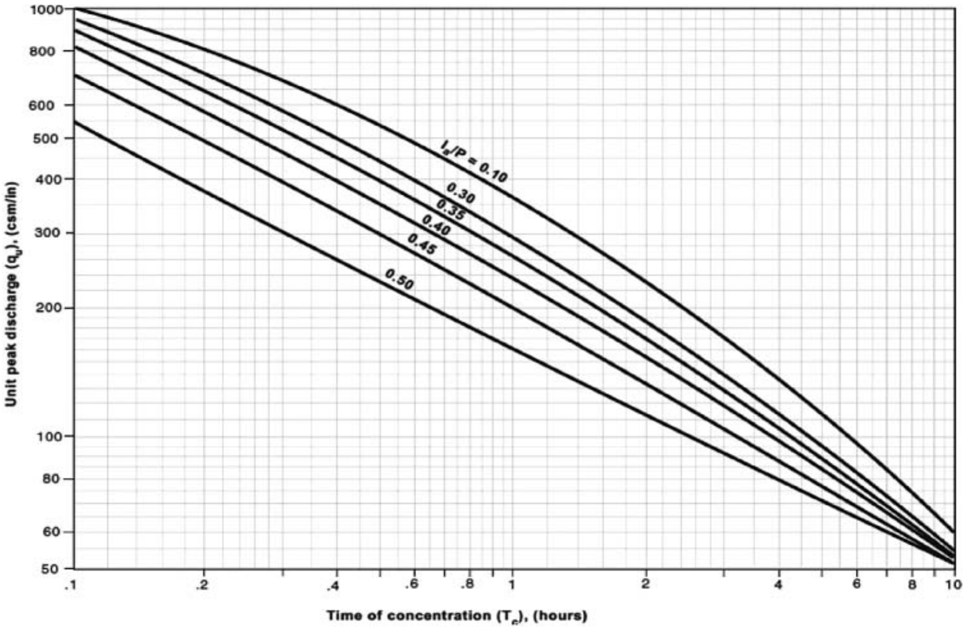

Figure 6. Unit peak discharge (q_u) for The U.S. Soil Conservation Service (SCS) type II rainfall distribution. Source: USDA (1986).

period) (A, C, b and n are based on specific weather for HCMC, and associated with a design rainfall event of 2 years (Cao 2011)), t = time of concentration (min).

Values of bankfull discharge were measured using Equation (10) with the concentration time calculated in Equation (8). The values of peak discharge calculated in Equation (9) were converted to m^3/s for comparing with values of bankfull discharge.

Once the values for bankfull discharge and peak discharge values were obtained for each sub-catchment, flood flows were calculated ($q_{\text{flood}} = q_p - q_b$) and then the runoff of flood (flood depth) was identified using Equation (9) by assuming Q as unknown. These values of flood depth of each sub-catchment formed the pixel values to create maps of rainfall induced flood.

2.2.5. Flood caused by tides

The definition of tidal flood was determined by overlaying and analysing two raster layers, DEM and river water level. The values of river water were transferred and stored in raster format using the 3D Analyst tools in ArcGIS (ESRI 2012), then the two raster layers were overlaid and analysed and corresponding pixels of the water level layer were subtracted from the DEM layer. In the results layer, pixels with positive values were at risk of flooding because they had higher water levels than the elevation. Conversely, pixels with negative or zero values were not flooded.

2.2.6. Overall flood map (flood map caused by rainfall and tides)

The overall flood map was produced using the Plus Tool (Analyst Tools) in ArcGIS (ESRI 2012). The overall flood raster map was created by summing the values of the rainfall-induced flood and tide-induced flood rasters on a cell-by-cell basis.

3. Results

The results indicate that a number of peak discharges exceeded the bankfull discharges in several sub-catchments, and so these sub-catchments are deemed to be subject to flooding (Table 3).

Table 3. Results of runoff, time of concentration, bankfull discharge and peak discharge for each sub-catchment in District 8, Ho Chi Minh City in 2010. Rows in bold show those sub-catchments where the peak discharge is greater than bankfull discharge.

Sub-catchment	Runoff (*Q*) (cm)	Concentration time (hour)	Peak discharge (m^3/s)	Bankfull discharge (m^3/s)
1	8.0076	0.8760	1.6907	6.4296
2	**7.8302**	**2.4063**	**3.2252**	**2.4770**
3	7.1250	1.7686	2.9230	3.3145
4	6.9439	1.5939	2.3834	3.6567
5	5.6698	2.3808	2.1836	2.5021
6	**6.8967**	**2.3483**	**4.0431**	**2.5349**
7	7.3753	1.6493	2.1855	3.5405
8	**7.2751**	**3.9541**	**2.7430**	**1.5474**
9	**7.0702**	**9.0052**	**2.7521**	**0.7088**
10	**6.8047**	**3.3660**	**5.4272**	**1.8025**
11	6.2280	1.4910	1.8951	3.8946
12	**8.1049**	**1.6962**	**4.8410**	**3.4479**
13	**5.7297**	**5.0911**	**2.6334**	**1.2177**
14	7.1683	3.1753	1.6554	1.9049
15	**6.6483**	**3.4528**	**2.3485**	**1.7596**
16	**6.1060**	**3.2732**	**2.8920**	**1.8509**
17	**7.0573**	**5.2480**	**2.2200**	**1.1831**
18	7.1498	1.3943	1.1295	4.1492
19	5.2160	3.5312	1.6499	1.7225
20	6.1080	4.4074	1.1395	1.3961
21	5.8055	4.7112	1.2697	1.3106
22	5.3003	2.7100	2.0675	2.2134
23	**6.2800**	**7.2955**	**1.9971**	**0.8656**
24	6.5565	2.4059	1.8573	2.4773
25	5.2782	2.0901	2.7240	2.8302
26	**5.9113**	**7.7410**	**2.5894**	**0.8183**
27	**5.3786**	**2.3278**	**2.5660**	**2.5560**
28	4.2716	2.0680	2.0899	2.8588
29	4.8315	1.2531	1.4786	4.5892
30	4.9765	1.8656	0.6402	3.1513

3.1. Flood risk maps

3.1.1. Map of floods caused by rainfall

Figure 7 shows the areas of District 8 of HCMC where rainfall-induced floods occurred in 2010 and also the level of the flooding based on the calculations in Table 3. Approximately 60% of the total area of District 8 was subject to flooding caused by rainfall. The results of this case study show that although much of the case study area is vulnerable to flooding, the depth of the flooding is minimal. In 2010, flood depths ranged from just 2 cm to just below 10 cm. Around 70% of the flooded area was flooded to a depth of less than 5 cm, with the remainder flooded to a depth of 5–10 cm. Additionally, the flooded areas and areas of high risk of flood with flood depth around 10 cm were located in the north-east (centre) of the district, in places with a high proportion of construction and transportation land use.

3.1.2. Map of floods caused by tides

District 8 is also subject to flooding caused by tides (Figure 8). In contrast with floods by rainfall, floods by tide typically occurred in the south-west of District 8, in areas where the elevation of the land was lower than the river water level when there was high tide. Approximately 60% of the total area of District 8 was flooded by tide. Flooding caused by tides was significantly greater than flooding caused by rainfall. Most areas were flooded to a depth of more than 10 cm by the tide, and in some areas the flood depth reached 100 cm.

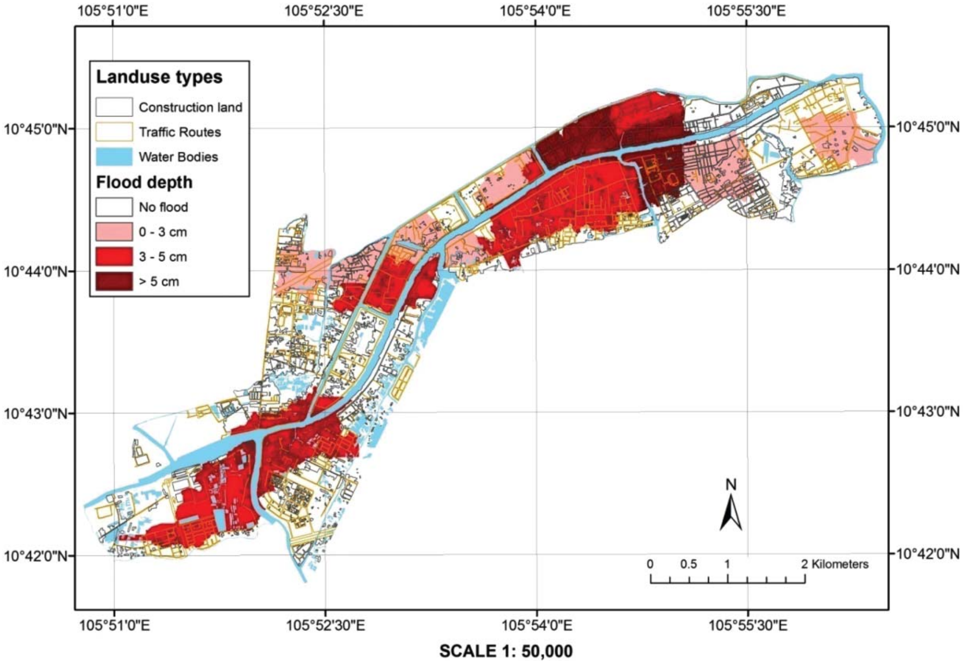

Figure 7. Map of simulated flooding caused by rainfall in District 8 of Ho Chi Minh City in the year 2010.

3.1.3. Map of flooding by both rainfall and tides

A flood map showing the combination of floods caused by both rainfall and tides is presented in Figure 9. The results of floods caused by a combination of rainfall and tides indicates that tides caused serious floods in the case study while rainfall was not a major contributor to severe flood risk in the district. Furthermore, the combination of flooding by both tide and rainfall means that approximately 80% of District 8 is susceptible to flooding, and in low-lying areas the flood depth could be as deep as 100 cm, mostly due to tidal effects.

3.2. Factors affecting flood risk in District 8, Ho Chi Minh city, Vietnam

3.2.1. Land-use/land-cover

Figure 10(a) shows the effects of LULC on runoff depth in the case study site. The results show that sub-catchments 1, 2, 3, 6, 7, 8, 10 and 12, which were composed of more than 80% impervious areas, and sub-catchments 16, 17, 23 and 26, where the percentage of water body areas was greater than 30%, shared high CN values and high runoff in comparison to other sub-catchments (Figure 10 (a1)). Additionally, the correlation coefficient between runoff and CN (Figure 10(a2)) with r^2 of +0.99 illustrates the strong correlation between these two variables.

The results reveal that impervious areas considerably affected the flood phenomenon in the case study. In fact, sub-catchments with more than 70% impervious areas generally have direct runoff values between 6.5 and 8.1 cm. Sub-catchment 12 consists of 91% impervious area, and had the highest runoff of all sub-catchments (8.1 cm), and had flood depth of 3.5 cm. Similarly, sub-catchment 8 consists of 90% impervious areas, and had a runoff value of 7.28 cm, and experienced flood depth of 3.17 cm. In contrast, sub-catchment 28 had the lowest direct runoff value of 4.31 cm and only around 20% impervious area (Figure 10(b1)), so this sub-catchment was not flooded. Therefore, sub-catchments with more impervious areas have higher runoff and so are more vulnerable to flooding. Moreover, the correlation coefficient between runoff and impervious areas (Figure 10

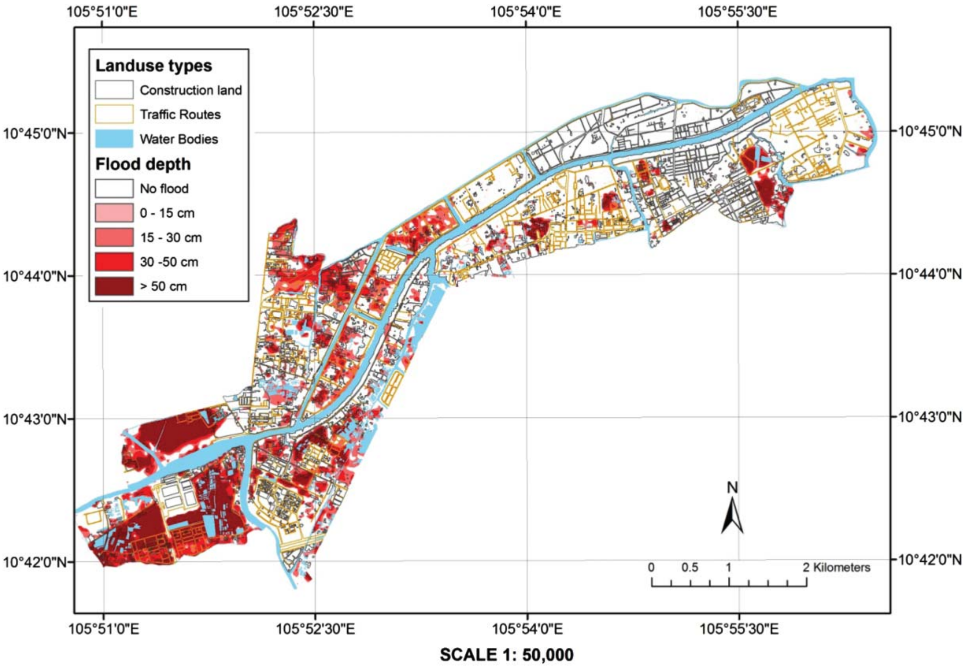
Landuse types
Construction land
Traffic Routes
Water Bodies
Flood depth
No flood
0 - 15 cm
15 - 30 cm
30 -50 cm
> 50 cm
105°51'0"E
105°52'30"E
105°54'0"E
105°55'30"E
10°45'0"N
10°44'0"N
10°43'0"N
10°42'0"N
N
0 0.5 1 2 Kilometers
SCALE 1: 50,000

Figure 8. Map of simulated flooding caused by tides in District 8 of Ho Chi Minh City in the year 2010.

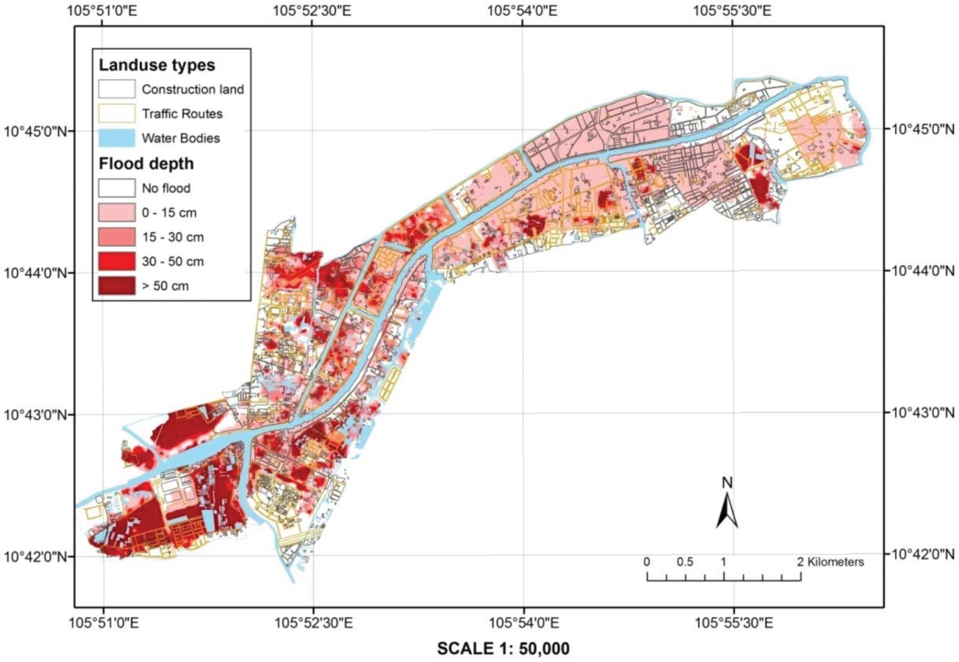
Landuse types
Construction land
Traffic Routes
Water Bodies
Flood depth
No flood
0 - 15 cm
15 - 30 cm
30 - 50 cm
> 50 cm
105°51'0"E
105°52'30"E
105°54'0"E
105°55'30"E
10°45'0"N
10°44'0"N
10°43'0"N
10°42'0"N
N
0 0.5 1 2 Kilometers
SCALE 1: 50,000

Figure 9. Map of simulated flooding caused by both rainfall and tides in District 8 of Ho Chi Minh City in the year 2010.

(b2)) with r^2 value of +0.73 indicates the strong correlation between these two variables, and this shows that an increase in impervious areas exacerbates flood risk in District 8.

3.2.2. Flow length of the catchment

In general, an extensive flow length led to decreased flood risk of sub-catchments in the case study (Figure 10(c)). Sub-catchments 1, 28 and 30, which had high flow lengths, had lower flood depth, and so were not susceptible to flooding. In contrast, sub-catchments with flow lengths less than 25 m/ha had high flood depth and were typically flooded (sub-catchments 2, 6, 8, 9, 12, etc.) (Figure 10(c1)). Furthermore, the correlation coefficient between runoff and impervious areas (Figure 10(c2)) with r^2 value of −0.86 confirmed the existence of a strong correlation between flow length of sub-catchments and flood risk, implying that a decrease in flow lengths (decrease in areas of canal and river) due to urbanization will increase flood phenomenon in the district.

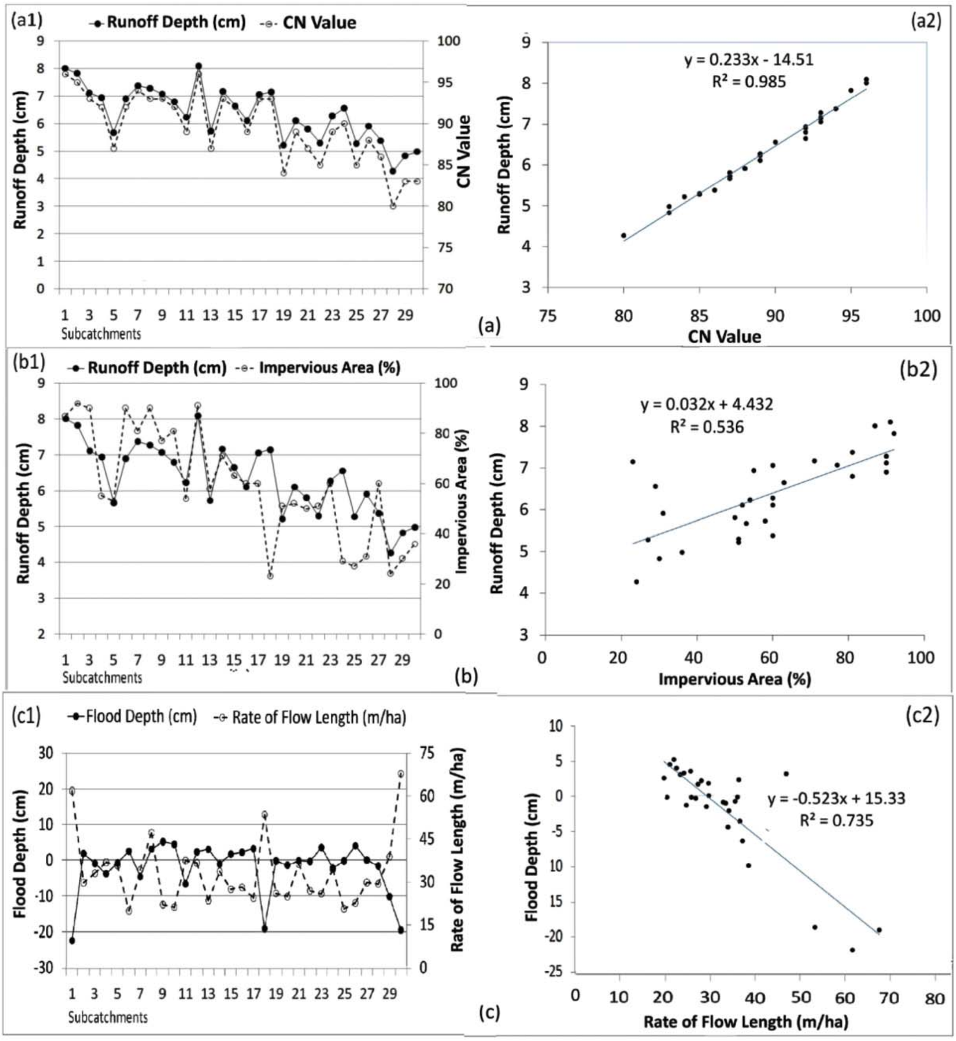

Figure 10. Factors impacting flood risk in District 8, Ho Chi Minh city: (a) the relationship between CN values (based on types of LULC) and runoff depth; (b) relationship between impervious area and runoff depth; (b) the relationship between flow length and flood depth.

4. Discussion

For the SCS method of predicting flooding, CN values are obtained from LULC features and vary with the type of LULC, so LULC plays a vital role in affecting and determining the runoff volume for sub-catchments. The results support the findings of Dawod et al. (2011) who also concluded that the higher the CN values of sub-catchments were, the higher the runoff and flood hazards.

The results imply that the increase of impervious areas leads to growing runoff volume, and so flood risk increases. This finding supports previous research results which indicated that impervious areas growth due to urbanization have considerable effect on the hydrological cycle, including increasing the runoff volume in urban sub-catchments(Camorani et al. 2005; Shuster et al. 2005; Brilly et al. 2006; Pappas et al. 2008; Gholami et al. 2010), thereby increasing flood risk. Moreover, a growth of both runoff volume and peak flow rates in urban areas due to urbanization usually leads to a subsequent increase in both the magnitude of floods and the occurrence of local flooding (Moscrip and Montgomery 1997; Doyle et al. 2000; Gholami et al. 2010).

This study also showed that increased flow length resulted in a decrease in peak discharge, and a reduction in flood risk. This may explain why some sub-catchments which had a lot of impervious areas were not flooded, for example sub-catchment 1. Dawod et al. (2011) concluded that flow length is one of the main factors affecting runoff and flood risk in urban areas. Long et al. (2010) argued that once flow length of sub-catchments increases, the values of bankfull discharge will be improved, and so the flood hazard will logically be reduced in areas with a high rate of flow length. This relationship also explains the situation in which rapid urbanization decreases the amount of drainage area and drainage capacities of existing canals leading to a reduction of flow length in urban areas, accelerating flood hazard (Long et al. 2010).

According to rainfall induced flood in District 8, areas of high risk of flood were highly developed and were characterized by a high proportion of construction and transportation land use. These areas, located in the centre of the district, are older in comparison to other areas, thereby infrastructure, such as pipe systems for discharging runoffs, are old and ineffective which accelerate flooding (Xuan 2014b). Some areas in the south-west of the district were also flooded despite having few impervious areas. This can be attributed to their low elevation and large number of water bodies, including intensive system of rivers and canals which contributes to increased runoff and flooding (Thanh Tu and Nitivattananon 2011; Xuan 2014a). The natural lowland with inadequate infrastructure system experiences serious floods when there is a combination of high tide and rainfall (Thanh Tu and Nitivattananon 2011).

Critically, the methods developed in our research show that RS techniques used for identifying rainfall-induced flood risk are effective in supporting hydrological models. RS techniques enable updating vital variables for flood risk analysis, such as LULC and especially impervious areas, extracted from satellite imagery. This overcomes the previous issue of a lack of up-to-date information on infrastructure for use in flood forecasting in HCMC (Lempert et al. 2013) and so enables flood phenomena to be predicted more accurately. This research also points out that the underlying factors leading to flooding in the case study include increased impervious area and decreased flow length, both due to increasing urban development. These findings are critical and need to be considered for informed decision-making and planning in flood risk prevention and management.

Relating to tide-induced floods, the method used was straightforward and simple, based on the ArcGIS Analyst Tool. Due to the simplicity of this method, the accuracy of the input data plays a vital role in producing an accurate result, particularly the quality of the DEM. The use of a DEM is considered to be the most effective means to estimate flood depth from remotely sensed or hydrological data (Seeni Mohd and Mansor 2000; Sanyal and Lu 2004). Tikkanen (2013) also found that this 2 m scale of DEM was successful in delineating sub-catchments and was reliable for extracting information supporting hydrological models for flood risk analysis. However, to improve the accuracy of results, Light Detection and Ranging (LiDAR) data should be used to create DEM as LiDAR data provide the opportunity to create high-quality DEMs with improved vertical accuracy (Isenburg et al. 2006; Sanders 2007; ESRI 2012).

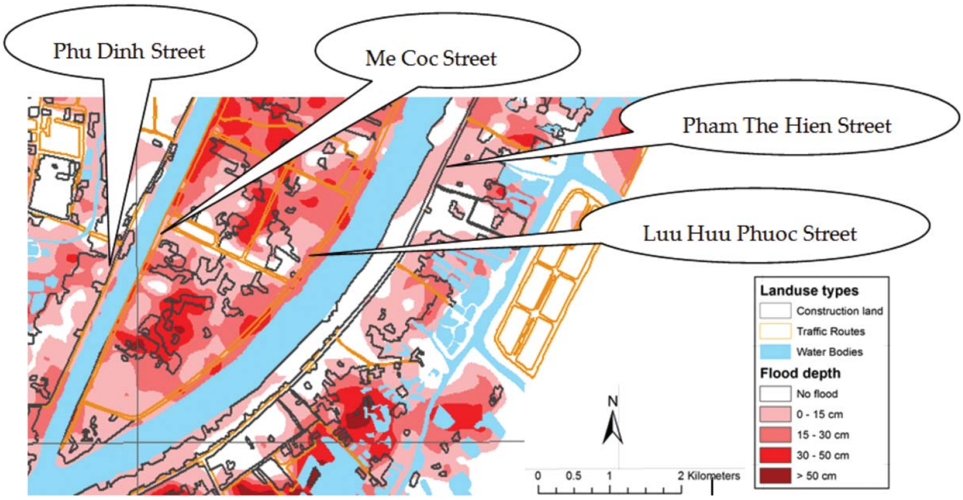

Figure 11. Validating some flooded areas in District 8, Ho Chi Minh City, Vietnam in 2010.

In our research, the reliability of the water level data collected from PhuAn meteorological station and a 2 m resolution DEM enabled highly accurate results. Indeed, the results of flood risk caused by tides closely match with observed data on flooding in HCMC. There are a number of locations along Sai Gon River (including District 8) that were flooded extensively with 40–80 cm in depth caused by tides (Tran 2011; Thanh Trung 2014). Importantly, many locations in low lying areas in HCMC are flooded with flood depths that peak up to above 100 cm due to tides (Ho 2008; Thanh Trung 2014). Our modelling predicts a number of low lying areas in District 8 that are subject to flooding, and these correspond with a number of floods caused by tides. These findings show that the method used is effective in predicting the cause of flooding and so could be utilized to assess the effects of sea level rises on flood risks in the city.

In terms of overall flooding, the findings correspond to documented and observed records, verifying the accuracy of the method developed in this study. Ho (2008) concluded that serious flood risk in HCMC is mostly caused by tides as during high tides the water infiltrates back up storm water conduits. These locations are also subjected to inundation frequently, even when the rainfall is not heavy (Storch 2008; Nguyen 2013). Approximately 60% of the city area is subjected to tidal flooding, resulting solely from monthly high tides (Storch 2008; Tran 2011). Some areas of District 8 are always flooded due to occurrence of high tides (Nguyen 2013). Additionally, intensive rainfall exacerbates flooding caused by tides at certain times of the year when the annual peak tidal period coincides with the annual peak in rainfall (Long 2007; Ho 2008; Tran 2011). Critically, the result of the overall flooding map should significantly contribute to flood risk management by identifying specific flooded areas and flood depths that were not previously undertaken in the case study.

Due to the limitations of data, in that there are no observed inundation maps in the case study, the results of flood maps could not be validated. However, according to a few reports, some areas along Me Coc, Pham The Hien, Luu Huu Phuoc, Phu Dinh street and residential areas surrounding these streets were flooded with flood depths ranging from 10 to around 30 cm due to a combination of high tide and heavy rainfall in 2010 (Nguyen 2011). Our results correspond to these observed data (Figure 11).

4.1. Limitations and uncertainty in this study

The SCS TR-55 model used to identify flood risk caused by rainfall was based on equations and variables developed using data from the United States. This is a limitation of the model as the values of some of the parameters of LULC and soil may not be transferable to Vietnam. Thus, the model needs to be calibrated and validated for use in other cities. Backwater is also a factor in flood modelling but we did not consider it in this study since we do not believe it will make a significant difference in the results. In our study site, which is relatively flat and the river slope is very low to negligible, we believe that backwater impacts would be negligible. The backwater effect is more of an issue in faster flowing river systems with higher slope gradients, and more so in upstream conditions. However, this could be tested in future research with further developments in the SCS-CN and SCS TR-55 models. The current models do not take this into account.

Additionally, analysis of the flooded areas and flood depth caused by tides was identified simply by comparing the elevation of land and water level in rivers using the ArcGIS tool. This method produced accurate results; however, there is still a need to calibrate the results by comparing calculated values with field observations over a longer time period and multiple flooding events.

5. Conclusions

This study developed methods to predict flood hazard in District 8, HCMC. Flooded areas and levels of flood caused by both rainfall and tidal effects in the case study site were projected based on current infrastructure (rapidly updated from remotely sensed data),as well as updated climate factors such as rainfall and sea level (previously not considered). Hence, the research contributes to solving the issue of a shortage of up-to-date information on infrastructure and climate conditions for use in flood forecasting, so as to enable flood phenomena to be predicted more accurately.

The maps of the flood prone areas and flood depth caused by both rainfall and tides provide a vital understanding of the areas of District 8 that are subject to flooding so that councils can work to reduce or prevent flooding in these areas. Tide-induced floods (flood depth ranged from 10 to around 100 cm) are a more significant issue than flooding by rainfall (flood depth of less than 10 cm). Therefore, preventing flooding by tides should be a primary objective for management. One of the most effective methods to do this is to improve storm water drainages so that they are above the high tide level and so prevent flooding. The risk maps produced are important for determining locations that are at high risk of flooding in order to prevent loss of life, minimize damage to property and support planning.

Growing urbanization increases impervious surface areas; this is an important factor contributing to increased flood risk in District 8. Hence, there needs to be schemes to manage urbanization processes that involve utilizing appropriate infrastructure to minimize the risk of flooding. Additionally, an increase in flow length of catchments will decrease runoff volume, and so a reduction of flood hazard. Therefore, improving the infiltration capacity and decreasing the water overflow in the urban landscape with optimized drainage systems will be an effective method to minimize and control flood risk in urban areas. These findings are critical to inform decision-makers and planning for flood risk prevention and management.

The methods developed in this study has the advantage of being cost-effective, precise, outputs are in a digital form and have the ability to re-use other LULC, rainfall and topography values, not only in other urban areas of Vietnam, but also across the whole world. The non-calibrated SCS TR-55 applications show promise for certain applications in using storm water modelling to evaluate flood risk in urban areas. However, further research on application of SCS TR-55 in flood risk analysis is still required, including calibrating the SCS TR-55 model and validating the results.

Acknowledgments

The authors gratefully acknowledge the School of Environmental and Rural Science at the University of New England, Australia for financial support. We appreciate data support from the Department of National Remote Sensing, MONRE, Vietnam. A. T. N. Dang would like to express her gratitude to her supervisor and parents for constant support during this study.

Disclosure statement

No potential conflict of interest was reported by the authors.

Funding

School of Environmental and Rural Science at the University of New England, Australia.

ORCID

Lalit Kumar http://orcid.org/0000-0002-9205-756X

References

Brilly M, Rusjan S, Vidmar A. 2006. Monitoring the impact of urbanisation on the Glinscica stream. Phys Chem Earth Parts A/B/C. 31:1089–1096.

Camorani G, Castellarin A, Brath A. 2005. Effects of land-use changes on the hydrologic response of reclamation systems. Phys Chem Earth Parts A/B/C. 30:561–574.

Cao DD. 2011. Survey research and flood warnings to support disaster prevention in the Central Basin. Ha Noi (Vietnam): Vietnam Academy of Science and Technology, Institute of Meteorology Hydrology and Climate Change.

Carew-Reid J. 2008. Rapid assessment of the extent and impact of sea level rise in Viet Nam. Brisbane: International Centre for Environment Management (ICEM); p. 82.

Chowdhury MR. 2000. An assessment of flood forecasting in Bangladesh: the experience of the 1998 flood. Nat Hazards. 22:139–163.

Dahm D. 2013. On the flood and inundation management of Ho Chi MInh City, Vietnam. Reino Unido: ICFR: Experiences in Asia and Europe.

Dano Umar L, Matori AN, Hashim AM, Chandio IA, Sabri S, Balogun AL, Abba HA. 2011. Geographic information system and remote sensing applications in flood hazards management: a review. Res J Appl Sci Eng Technol. 3:933–947.

Dawod GM, Mirza MN, Al-Ghamdi KA. 2011. GIS-based spatial mapping of flash flood hazard in Makkah City, Saudi Arabia. JGIS. 03:225–230.

Department of Water Sanitation and Environment. 2008. Vietnamese environmental standard no. 7957 (TCVN 7957). Ha Noi (Vietnam): Vietnamese Government, Ministry of Science and Technology.

Doyle MW, Harbor JM, Rich CF, Spacie A. 2000. Examining the effects of urbanization on streams using indicators of geomorphic stability. Phys Geogr. 21:155–181.

Eckert R. 2011. Guidelines and rating systems as tools to foster climate change adaptation of Ho Chi Minh City's urban infrastructure. Paper presented at: REAL CORP Tagungsband; May 18–20; Essen, Germany.

ESRI. 2012. 10.1 CA. Redlands: Environmental Systems Research Institute.

Field CB. 2012. Summary for policymakers. In: Field CB, editor. Managing the risks of extreme events and disasters to advance climate change. Adaptation (UK): Cambridge University Press.

Fleming M, Doan J. 2009. HEC-GeoHMS geospatial hydrologic modelling extension: user's manual version 4.2. California: US Army Corps of Engineers, Institute for Water Resources, Hydrologic Engineering Centre.

Gajbhiye S, Mishra S. 2012. Application of NRSC-SCS curve number model in runoff estimation using RS & GIS. Proceedings of the 2012 International Conference on Advances in Engineering, Science and Management; Mar 30–31; Tamil Nadu, India. IEEE.

Gallegos HA, Schubert JE, Sanders BF. 2009. Two-dimensional, high-resolution modeling of urban dam-break flooding: a case study of Baldwin Hills, California. Adv Water Resour. 32:1323–1335.

Gholami V, Mohseni Saravi M, Ahmadi H. 2010. Effects of impervious surfaces and urban development on runoff generation and flood hazard in the Hajighoshan watershed. Caspian J Environ Sci. 8:1–12.

Hallegatte S, Green C, Nicholls RJ, Corfee-Morlot J. 2013. Future flood losses in major coastal cities. Nat Clim Change. 3:802–806.

Hanson S, Nicholls R, Ranger N, Hallegatte S, Corfee-Morlot J, Herweijer C, Chateau J. 2011. A global ranking of port cities with high exposure to climate extremes. Clim Change. 104:89–111.

Ho LP. 2008. Impacts of climate changes and urbanisation on urban inundation in Ho Chi Minh City. Proceedings of the 11th International Conference on Urban Drainage; 31 Aug–5 Sep; Scotland (UK). IAHR/IWA.

Holman–Dodds JK, Bradley AA, Potter KW. 2003. Evaluation of hydrologic benefits of infiltration based on urban storm water management. J Am Water Resour Assoc. 39:205–215.

Huong H, Pathirana A. 2013. Urbanization and climate change impacts on future urban flooding in Can Tho city, Vietnam. Hydrol Earth Syst Sci. 17:379–394.

Isenburg M, Liu Y, Shewchuk J, Snoeyink J, Thirion T. 2006. Generating raster DEM from mass points via TIN streaming. Munster (Germany): Springer.

Isma'il M, Opeluwa Saanyol I. 2013. Application of remote sensing (RS) and geographic information systems (GIS) in flood vulnerability mapping: case study of River Kaduna. Int J Geomat Geosci. 3:618–627.

Kim NW, Lee JW, Lee J, Lee JE. 2010. SWAT application to estimate design runoff curve number for South Korean conditions. Hydrol Process. 24:2156–2170.

Lempert R, Kalra N, Peyraud S, Mao Z, Tan SB, Cira D, Lotsch A. 2013. Ensuring robust flood risk management in Ho Chi Minh city. World Bank Policy Res Working Paper. 6465:1–63.

Long PH. 2007. Climate change and urban flooding in Ho Chi Minh City. Proceedings of 3rd International Conference on Climate and Water; Sep 3–6; Helsinki (Finland). Finnish Environment Institute.

Long BT, Hoa NT, Khai NN. 2010. Evaluation and forecasting flooding in Ho Chi Minh City using mike flood model. Paper presented at: GeoInformatics for Spatial-Infrastructure Development in Earth and Allied Sciences (GIS-IDEAS); Dec 9–11; Hanoi, Vietnam.

Merwade V, Cook A, Coonrod J. 2008. GIS techniques for creating river terrain models for hydrodynamic modeling and flood inundation mapping. Environ Modelling Softw. 23:1300–1311.

Moscrip AL, Montgomery DR. 1997. Urbanization flood, frequency and salmon abundance in Puget Lowlan Streams. J Am Water Resour Assoc. 33:1289–1297.

Nguyen NC. 2011. Comparison of serious flood areas caused by heavy rainfall and high tides from 2008 to 2011. Ho Chi Minh City (Vietnam): Vietnam People's Committee of Ho Chi Minh City.

Nguyen D. 2013. Flooding caused by tides in Ho Chi Minh City [Internet]. Tien Phong Newspaper. [updated 2013 Dec 18; cited 2014 May 20]. Ho Chi Minh City. http://wwwtienphongvn/xa-hoi/trieu-cuong-gay-ngap-lut-tai-tphcm-tu-chong-sang-song-chung-663878tpo.

Nguyen MH, Tung ST. 2007. Governance screening for urban climate change resilience-building and adaptation strategies in Asia: assessment of Ho Chi Minh City, Vietnam. Brighton (UK): University of Sussex, Institute of Development Studies (IDS).

Nicandrou A. 2011. Hydrological assessment and modelling of the River Fani Catchment, Albania [dissertation]. London (UK): University of Glamorgan.

Nicandrou A, Mofor LA, Delpak R, Robinson RB. 2004. Hydrological assessment and modeling of the River Fani catchment in Albania using GIS and remote sensing. Remote Sens Agric Ecosyst Hydrol V. 5232:340–350.

Nicholls RJ, Hanson S, Herweijer C, Patmore N, Hallegatte S, Corfee-Morlot J, Chateau J, Muir-Wood R. 2008. Ranking port cities with high exposure and vulnerability to climate extremes, exposure estimates. Environment Working Papers 1. France: OECD.

Pappas E, Smith D, Huang C, Shuster W, Bonta J. 2008. Impervious surface impacts to runoff and sediment discharge under laboratory rainfall simulation. Catena. 72:146–152.

Ramana GV. 2014. Rainfall runoff modeling between TR-55 hydrologic watershed model and overland time of concentration model. Int J. 3:220–241.

Samarasinghea S, Nandalalb H, Weliwitiyac D, Fowzed J, Hazarikad M, Samarakoond L. 2010. Application of remote sensing and GIS for flood risk analysis: a case study at Kalu-Ganga River, Sri Lanka. Int Arch Photogramm Remote Sens Spatial Inform Sci. 38:110–115.

Sanders BF. 2007. Evaluation of on-line DEMs for flood inundation modeling. Adv Water Resour. 30:1831–1843.

Sanyal J, Lu XX. 2004. Application of remote sensing in flood management with special reference to Monsoon Asia: a review. Nat Hazards. 33:283–301.

Sarker MZ, Sivertun Å. 2011. GIS and RS combined analysis for flood prediction mapping – a case study of Dhaka City Corporation, Bangladesh. J Electr Control Eng. 1:250–257.

Sdao F, Sole A, Sivertun Å, Albano R, Giosa L, Pascale S. 2010. Implementation in a GIS environment of a systemic vulnerability assessment model. Proceedings of the 6th National Conference on Computer Science and Urban and Territorial Planning (INPUT 2001); Sep 13–15. Potenza (Italia): Campus of Macchia Romana.

Seeni Mohd I, Mansor MA. 2000. Application of remote sensing and hydrological modelling in flood prediction studies. Malaysian J Remote Sens GIS. 1:91–98.

Shadeed S, Almasri M. 2010. Application of GIS-based SCS-CN method in West Bank catchments, Palestine. Water Sci Eng. 3:1–13.

Shen J, Parker A, Riverson J. 2005. A new approach for a windows-based watershed modeling system based on a database-supporting architecture. Environ Modelling Softw. 20:1127–1138.

Shuster W, Bonta J, Thurston H, Warnemuende E, Smith D. 2005. Impacts of impervious surface on watershed hydrology: a review. Urban Water J. 2:263–275.

Siart C, Bubenzer O, Eitel B. 2009. Combining digital elevation data (SRTM/ASTER), high resolution satellite imagery (Quickbird) and GIS for geomorphological mapping: a multi-component case study on Mediterranean karst in Central Crete. Geomorphology. 112:106–121.

Sivertun Å, Prange L. 2003. Non-point source critical area analysis in the Gisselö watershed using GIS. Environ Modelling Softw. 18:887–898.

Soulis K, Valiantzas J. 2011. SCS-CN parameter determination using rainfall-runoff data in heterogeneous watersheds – the two-CN system approach. Hydrol Earth Syst Sci Discuss. 8:8963–9004.

Storch H. 2008. Adapting Ho Chi Minh City for climate change. Urban compactness: a problem or a solution. Proceedings of the 44th ISOCARP Congress; Sep 19–23. Dalian (China): ISOCARP.

Storch H, Downes NK. 2011. A scenario-based approach to assess Ho Chi Minh City's urban development strategies against the impact of climate change. Cities. 28:517–526.

Tarboton DG, Ames DP. 2001. Advances in the mapping of flow networks from digital elevation data. Proceedings of the World Water And Environmental Resources Congress; May 20–24. Florida: American Society of Civil Engineers.

Thanh Trung. 2014. More than 50 locations of serious flooding by high tides in Ho Chi Minh City [Internet]. Ho Chi Minh City: VOV (Radio the Voice of Vietnam); [updated 2014 Oct 9; cited 2014 May 20]. http://vovvn/doi-song/hon-50-diem-o-tp-hcm-ngap-nang-do-trieu-cuong-356974vov

Thanh Tu T, Nitivattananon V. 2011. Adaptation to flood risks in Ho Chi Minh City, Vietnam. Int J Clim Change Strateg Manage. 3:61–73.

Tianhong L, Yanxin S, An X. 2003. Integration of large scale fertilizing models with GIS using minimum unit. Environ Modelling Softw. 18:221–229.

Tikkanen H. 2013. Hydrological modeling of a large urban catchment using a stormwater [dissertation]. Helsinki (Finland): Aalto University.

Tran DH. 2011. Flooding in Ho Chi Minh City. Dong Nai & Cuu Long Cultural Research Organization Incorporated; p. 174–187.

Uddin K, Gurung DR, Giriraj A, Shrestha B. 2013. Application of remote sensing and GIS for flood hazard management: a case study from Sindh Province, Pakistan. Am J Geogr Inform Syst. 2:1–5.

[USDA] United States Department of Agriculture. 1986. Urban hydrology for small watersheds. Technical Release (TR-55). Washington, DC: Department of Agriculture, Soil Conservation Service, Engineering Division.

Vietnam GIS. 2014. The maps of 63 provinces in Vietnam [Internet]. Hanoi (Vietnam): Government Organization: Vietnam GIS Government; [updated 2010 May 22; cited 2014 April 20] http://gischinhphuvn/

Vo QT, Oppelt N, Leinenkugel P, Kuenzer C. 2013. Remote sensing in mapping mangrove ecosystems – an object-based approach. Remote Sens. 5:183–201.

Wang X, Gu X, Wu Z, Wang C. 2010. Simulation of flood inundation of Guiyang city using remote sensing, GIS and hydrologic model. Int Arch Photogramm Remote Sens Spatial Inform Sci. 37:775–778.

Xuan H. 2014a. Geography and natural resources of district 8, Ho Chi Minh City [Internet]. Ho Chi Minh City: Vietnam People's Committee of District 8; [updated 2016 Sep 20; cited 2014 April 20]. http://www.quan8.hochiminhcity.gov.vn/pages/dieu-kien-tu-nhien.aspx

Xuan H. 2014b. Landuse planning of District 8, Ho Chi Minh city [Internet]. Ho Chi Minh City: Vietnam People's Committee of District 8; [updated 2013 Nov 22; cited 2014 May 20]. http://www.quan8.hochiminhcity.gov.vn/quyhoachphattrien/lists/posts/post.aspx?Source = /quyhoachphattrien&Category = Quy+ho%e1%ba%a1ch+%26+K%e1%ba%bf+ho%e1%ba%a1ch+s%e1%bb%ad+d%e1%bb%a5ng+%c4%91%e1%ba%a5t&ItemID = 10&Mode = 1.

© 2017 The Author(s). Published by Informa UK Limited, trading as Taylor and Francis Group. This work is licensed under the Creative Commons Attribution License creativecommons.org/licenses/by/4.0/ (the "License"). Notwithstanding the ProQuest Terms and Conditions, you may use this content in accordance with the terms of the License.